Nonlinear and Sequentially Linear Analysis of Tensile Strain Hardening Cement-based Composite Beams in Flexure

S.L. Billington
Stanford University,
Delft University of Technology, Faculty of Civil Engineering and Geosciences, Delft, The Netherlands

Keywords: engineered cementitious composites, flexure, nonlinear finite element analysis, smeared cracking, sequentially linear analysis, sawtooth

1 INTRODUCTION

High performance fiber reinforced cement-based composite (HPFRCC) materials have unique properties that are advantageous for many structural applications. In direct tension these materials can reach strains between 0.5% and 6% depending on material and specimen geometry. The large tensile strain capacity allows these materials to strain compatibly with steel reinforcement and achieve higher tension stiffening than traditional reinforced concrete. In compression, HPFRCC materials experience little to no spalling.

Currently there is little guidance on how to design with these materials in codes and specifications. To understand and explore more fully the potential benefits of such materials in structural applications, numerical modeling can be used. Both nonlinear finite element analysis as well as sequential linear analysis, the latter being particularly well suited for large-scale structural analyses (Rots and Invernizzi, 2004), can be used to evaluate HPFRCC material performance. In this presentation, a comparative analysis of small-scale slender beams made of engineered cementitious composites (ECC), a class of high performance fiber-reinforced cement-based composite, tested in four-point bending is made using nonlinear analysis with smeared cracking and using sequentially linear analysis. The nonlinear finite element analysis uses a total strain-based, smeared cracking model (Feenstra et al., 1998), which has proven effective in capturing global load-displacement behavior of structural-scale experiments well (e.g. Lee and Billington, 2008). The sequentially linear analysis uses a sawtooth softening crack model (Rots & Invernizzi, 2004).

2 EXPERIMENTS

The ECC for the beam experiments uses Type I/II Portland Cement, Class F fly ash, F110 Silica Sand, and water at the following weight ratios: 1:1.2:0.8:0.51. A high range water-reducing (HRWR) admixture is used (0.033 by weight of cement) and the fibers are polyvinyl alcohol (PVA), 0.5 in. (12.7mm) long, have a diameter of 0.0015 in. (0.038mm), and comprise 2% by volume of the total mix. The beams were tested in 4-point bending (i.e. simply-supported with two, equally-spaced point loads) as shown in Figure 1 and displacement was measured at mid-span. All specimens were tested in a table-top testing machine designed for educational use that loaded the specimens at a constant, quasi-static displacement rate where displacement was measured under a central loading point (between the point loads shown in Figure 1).

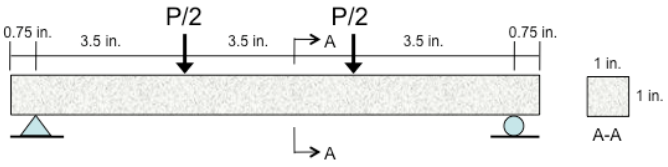

Figure 1. Beam Specimens *(1 in. = 25.4 mm)*

3 SIMULATIONS

For the nonlinear analyses, two-dimensional, 8-noded, plane stress elements of constant thickness and a 3x3 Gaussian integration scheme were used to model half of the beam with 4 elements along the height and 24 along the length. The ECC was modeled as linear elastic in compression as no softening in compression was expected nor observed in the experiments. Young's modulus was measured from an average of 4 cylinders tested in compression to be E=1,600 ksi (11,032 MPa). A total strain-based fixed crack model (Feenstra et al., 1998) was used with a tri-linear tensile stress-strain response assumed based on previous tensile tests of ECC dogbone specimens and defined by the following four stress-strain points: 1) (0,0), 2) (450 psi (3.1 MPa), 0.000281), 3) (600 psi (4.1 MPa), 0.025), and 4) (0, 0.05). A shear retention factor of 0.05 was used for the cracking and Poisson's ratio was taken as 0.15. The analyses were run in displacement control with a step size of 0.002 in. (0.05 mm) for 100 steps followed by 100 steps of 0.001 in. (0.025 mm), all applied at the loading point. The nonlinear analyses used a regular Newton-Raphson iteration scheme, including line estimation, with a maximum number of iterations of 30. Both a displacement and force tolerance of 1% were used for the convergence criteria.

For the sequential linear analyses, the same finite element model for the nonlinear analysis for half of the beam was used as described above, with the exception of using a 2x2 integration scheme rather than 3x3 in the elements. The ECC was modeled as linear elastic in compression as no softening in compression was expected nor observed in the experiments. Young's modulus was measured from an average of 4 cylinders tested in compression to be E=1,600 ksi (11,032 MPa). In tension, the same multi-linear tensile stress-strain curve from the nonlinear analysis was adopted for the baseline curve. To preserve fracture energy dissipation, a sawtooth model using an upper and lower bound curve, relative to the baseline curve, was adopted as shown in Figure 2. The upper and lower bound curves for the tension hardening and tension softening regions have the same stiffness as the baseline curve and represent a roughly 15% increase and decrease in stress at first cracking and peak cracking strength. Twenty stiffness reductions (similar to damage states) resulted to represent the full stress strain response. The grey triangles in Figure 2 highlight the preservation of fracture energy dissipation using the sawtooth model, whereby the triangle above the baseline curve is "extra" energy dissipated by loading along E2 up to the upperbound curve, and the triangle below the curve is the "missing" energy dissipation upon reloading along E3, again to the upperbound curve. These two triangles are roughly equal, thus allowing for the preservation of fracture energy dissipation with reasonable accuracy. Again, a shear retention factor of 0.05 was adopted and Poisson's ratio was taken as 0.15. The linear analyses were run in load control as explained above and were repeated for 2000 steps.

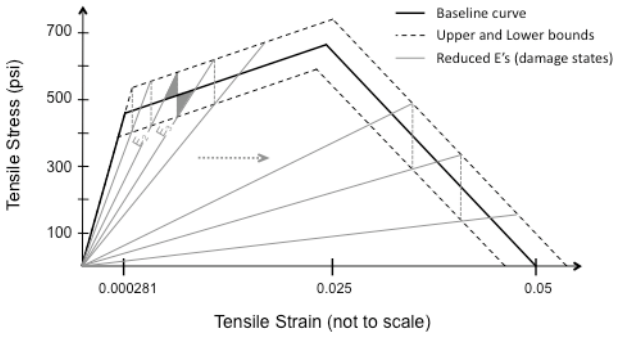

Figure 2. Saw-tooth tensile hardening-softening model for ECC *(100 psi =0.69MPa)*

Figure 3 compares the load-displacement response of the nonlinear analysis, the sequentially linear analysis and the three experiments on the ECC beams. The nonlinear analysis failed to converge in the second step after the peak load was reached (i.e. at a load of 141 lbs (627 N) and displacement of 0.25 in. (6.4

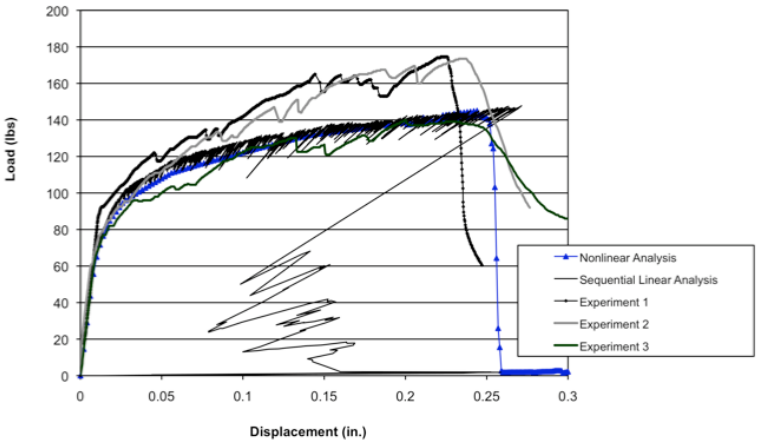

Figure 3. Load vs. Displacement of ECC beams and Analyses (*1 in. = 25.4 mm; 1 lb = 4.45 N)*

mm) and did not converge again until the load was essentially zero. This point of lack of convergence coincided with the first integration point to reach the softening branch of the ECC constitutive model. The sequential linear analysis is able to capture the likely snap-back experienced during failure. The test set-up was not able to capture snapback and therefore direct comparisons cannot be made.

Figure 4 compares the principal tensile strain contours at the last converged step at a load of 141 lbs (627 N) and displacement of 0.25 in. (6.4 mm) in the nonlinear analysis and at the same displacement and load pair for the sequentially linear analysis. The colors in Figure 4 represent different regions in the ECC tensile strain response as labeled in the figure. Both analysis methods show that at this displacement, the ECC has experienced significant multiple cracking and is just beginning to reach the softening branch.

Figure 5 shows the same principal tensile strain contours after the load has reduced to zero for each analysis method (and at equal displacements) with the same contour definitions as in Figure 4. Here it can be seen that a single, dominant crack has formed in the ECC in the constant moment region for each beam, although in slightly different locations, to roughly the same extent (height). Furthermore it can be seen in both analysis methods that as the ECC begins to form one dominant crack, the rest of the beam unloads and some of the previously cracked (hardening) region now experiences only elastic strain levels. Such unloading and closing of cracks is also observed experimentally.

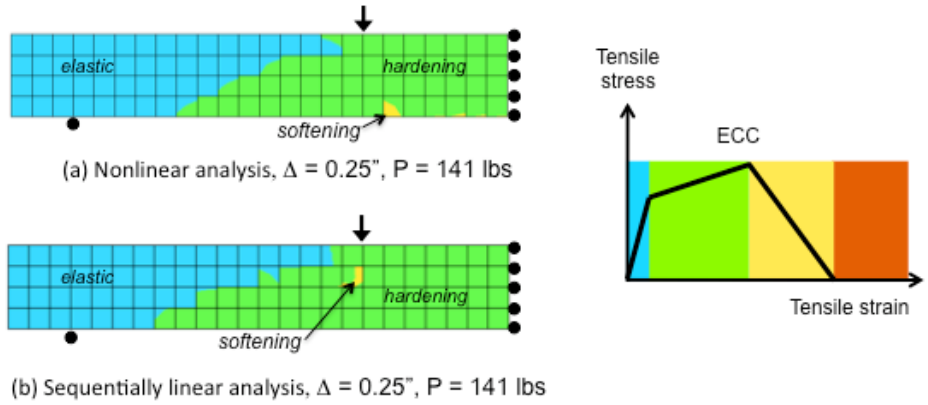

Figure 4. Principal tensile strain contours in ECC beams at last converged step for the nonlinear analysis *(1 in. = 25.4 mm; 1 lb = 4.45 N)*

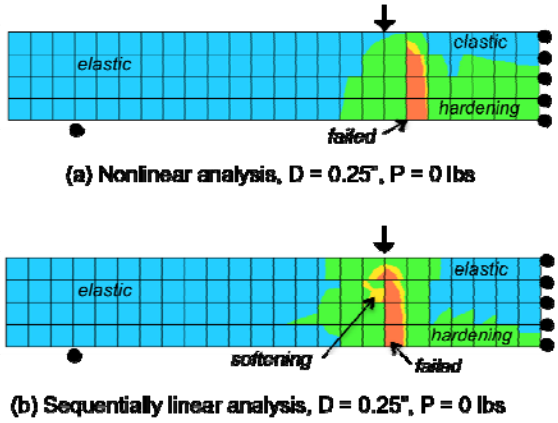

Figure 5. Principal tensile strain contours in ECC beams at failure ***(1 in. = 25.4 mm; 1 lb = 4.45 N)***

In Figure 6, the mesh sensitivity of the sequentially linear analysis is observed when comparing the original analysis (mesh of Figures 4-5) with an analysis performed on a beam with twice as many elements in each direction. Adopting the same saw-tooth softening model as for the original mesh, one would expect to see a more brittle response using the fine mesh, which is observed in Figure 6. A regularization procedure for tensile hardening-softening materials is needed.

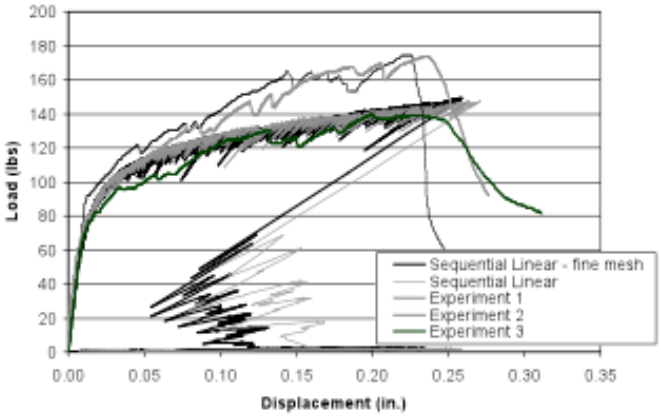

Figure 6. Load vs. Displacement of ECC beams from sequential linear analysis and two mesh sizes. *(1 in. = 25.4 mm; 1 lb = 4.45 N)*

4 SUMMARY & CONCLUSIONS

The flexural response of small-scale beams of ECC were simulated using two different analysis methods: nonlinear finite element analysis with a smeared, fixed crack model based on total strain, and sequential linear finite element analysis. It was found that both the nonlinear and sequential linear analysis methods predict well the load-displacement response of the deflection hardening ECC beams, using a tensile hardening-softening crack model. In both analyses, similar extents of multiple cracking were observed and softening of the ECC began at the same displacement (and load). A single, localized crack formed in both analyses to the same extent although in slightly different locations within the constant-moment region. Upon localization of the single dominant crack and unloading of the beam, the regions of the beam that had been tensile-hardening also unloaded in both analyses, as observed in experiments.

The sequential linear analysis was able to capture likely snapback behavior after crack localization. In the nonlinear analysis, a more advanced solution procedure would be required to capture the snap back. Measuring snap back in the experiments was not attempted, and further effort to capture this behavior in the nonlinear analysis was not pursued here. Mesh dependence was observed in the sequential linear analysis for the ECC beams, as the adopted crack model was not regularized for mesh size. A regularization procedure for tensile hardening-softening materials is required.

5 REFERENCES

Feenstra, P.H., Rots, J.G., Arnesen A., Teigen, J.G., Hoiseth, K.V. (1998) "A 3D constitutive model for concrete based on a con-rotational concept," *Computational Modelling of Concrete Structures, Proceedings of EURO-C 1998*, de Borst, Bicanic, Mang & Meschke (eds), Balkema, Rotterdam, 13-22.

Lee, W.K. and S.L. Billington (2008) "Simulation of Self-Centering Fiber-Reinforced Concrete Columns," *Proceedings of ICE, Engineering and Computational Mechanics*, **161**(2): 77-84.

Rots, J.G. and S. Invernizzi (2004) "Regularized sequentially linear saw-tooth softening model." *International Journal for Numerical and Analytical Methods in Geomechanics*, **28**:821-856.

Rots, J.G., Belletti, B., and S. Invernizzi (2006) "Event-by-event strategies for modelling concrete structures," *Computational Modelling of Concrete Structures, Proceedings of EURO-C 2006* Meschke, de Borst, Mang & Bicanic (eds), Taylor & Francis Group, London, 667-678.